Experimental and numerical study on mechanical properties of cement paste pipes subjected to uniaxial tensile loading

Ma, Xu; Schlangen, Erik; Çopuroğlu, Oğuzhan

DOI
10.1016/j.tafmec.2019.102296

Publication date
2019

Document Version
Final published version

Published in
Theoretical and Applied Fracture Mechanics

Theoretical and Applied Fracture Mechanics 103 (2019) 102296

Contents lists available at ScienceDirect

Theoretical and Applied Fracture Mechanics

journal homepage: www.elsevier.com/locate/tafmec

Experimental and numerical study on mechanical properties of cement paste pipes subjected to uniaxial tensile loading

Xu Ma, Erik Schlangen*, Oğuzhan Çopuroğlu

Microlab, Faculty of Civil Engineering and Geosciences, Delft University of Technology, 2628 CN Delft, the Netherlands

ARTICLE INFO

Keywords:
Uniaxial tensile test
Cement paste pipe
Single notch
3D lattice modeling
Mechanical properties

ABSTRACT

The aim of this paper is to investigate the mechanical properties of cement paste specimens by both experimental and numerical methods. Firstly, the specimens subjected to uniaxial tensile loading were studied experimentally. Afterwards, numerical investigation was carried out based on the experimental observations. Two types of specimens were used, which were unnotched and single notched specimens. The uniaxial tensile experiments of the unnotched specimens provided the Young's modulus and tensile strength of the specimens. The complete stress-strain responses of the specimens were derived from the uniaxial tensile experiments on the single notched specimens. The crack initiation and propagation were discussed.

The uniaxial tensile loading experiments were simulated by a 3D lattice model. The local mechanical properties of lattice elements were determined through simulations. The tensile simulations of the unnotched specimen provided the Young's modulus and tensile strength for the local lattice elements. Then, the softening behavior of lattice elements was obtained from tensile simulations of the single notched specimen. The experimental and simulated stress-strain responses and cracking process were compared with each other. It was found that the simulated results matched quite well with the experiments with the set of local mechanical properties that was determined. This set was used in a further study for the simulations on external sulfate attack.

1. Introduction

Concrete is a multiscale heterogeneous construction material. The mechanical performance of the material structure is determined by the distribution of the components, and the local mechanical properties of an individual component. They can be measured in the laboratory, as well as be simulated by a computational model. Cement paste is the basic binding material in concrete. Therefore, its mechanical properties have generated considerable research interest, such as tensile strength and constitutive response, which are the basic information for concrete structure design and durability investigation.

The direct way to obtain these mechanical properties is to perform experiments. A uniaxial (direct) tension test is thought to be the most direct method of determining the mode I fracture properties of concrete [1]. However, in the literature, the uniaxial tensile experiment of cement paste specimens is rarely studied. Toutanji et al. [2] tested the cylindrical specimens with a diameter of 16 mm and a length of 120 mm in uniaxial tension. The tensile strength of 8.8 MPa and 9.8 MPa were obtained for the cement paste specimens with a water/cement ratio of 0.31 and 0.28, respectively. In addition, for the cement paste specimens, the complete stress-strain curve including softening properties is missing in the literature. The application of fracture mechanics for the analysis of concrete structures requires the softening properties of the cementitious materials as an input parameter [1]. Therefore, this study focuses on the complete stress-strain curve of the specimens subjected to uniaxial tensile loading. Cement paste pipes with a wall thickness of 2.5 mm and a water/cement ratio of 0.40 were chosen.

In order to obtain a complete stress-strain curve for brittle material in uniaxial tension, it is essential to eliminate occurrence of sudden failure close to the peak stress [3,4]. One of the methods to address this issue is introducing a single notch on the specimen [5,6]. Therefore, the single notched specimens were chosen in order to make it possible for measuring the post-peak stress-strain curve of the specimens during experiments, which can trigger crack growth from a known location [5]. Previous experiments showed that crack nucleation and growth happens at the notch due to stress concentration [7]. As a result, in this study, two types of specimens were chosen for uniaxial tensile experiments, which were the unnotched and single notched cement paste pipes.

* Corresponding author.
E-mail address: Erik.Schlangen@tudelft.nl (E. Schlangen).

https://doi.org/10.1016/j.tafmec.2019.102296

Available online 06 July 2019

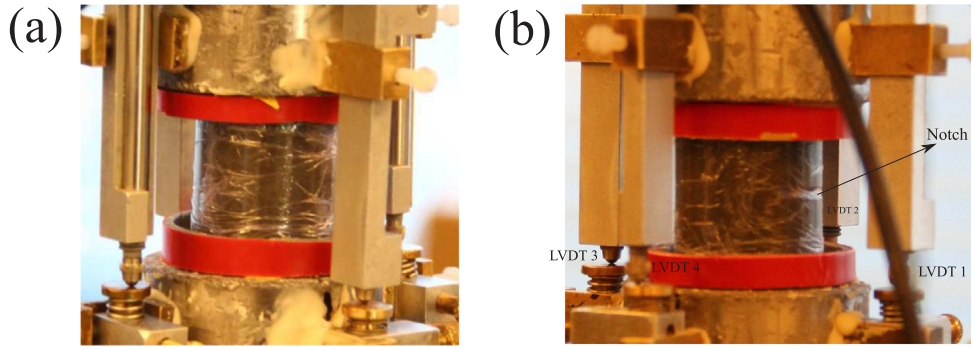

Fig. 1. Setup of uniaxial tensile tests. (a) An unnotched cement paste pipe and (b) a single notched cement paste pipe.

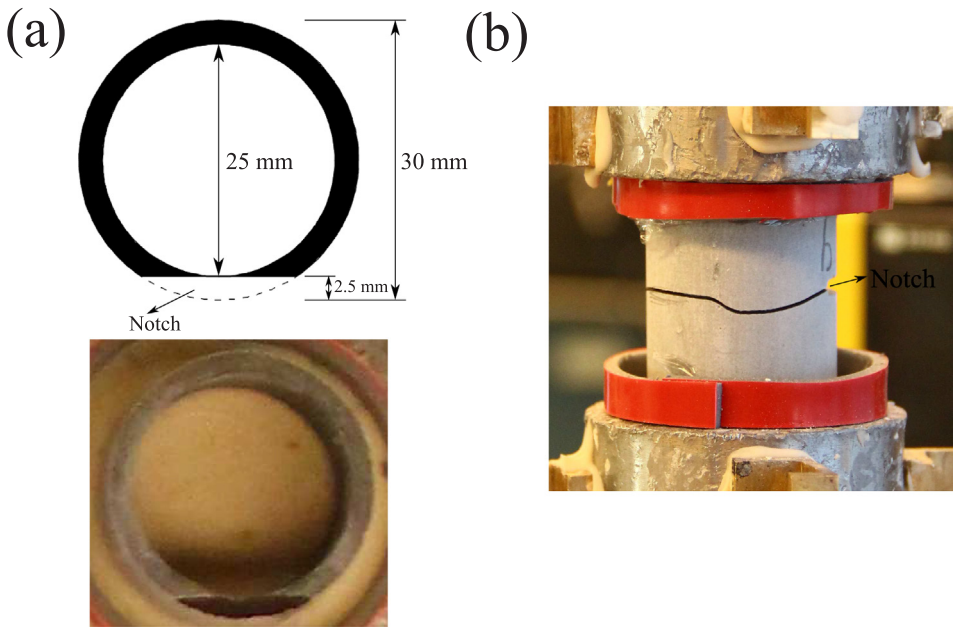

Fig. 2. Uniaxial tensile test of single notched cement paste pipes (Fig. 1b). (a) Geometric size of the notch and (b) cracked specimen.

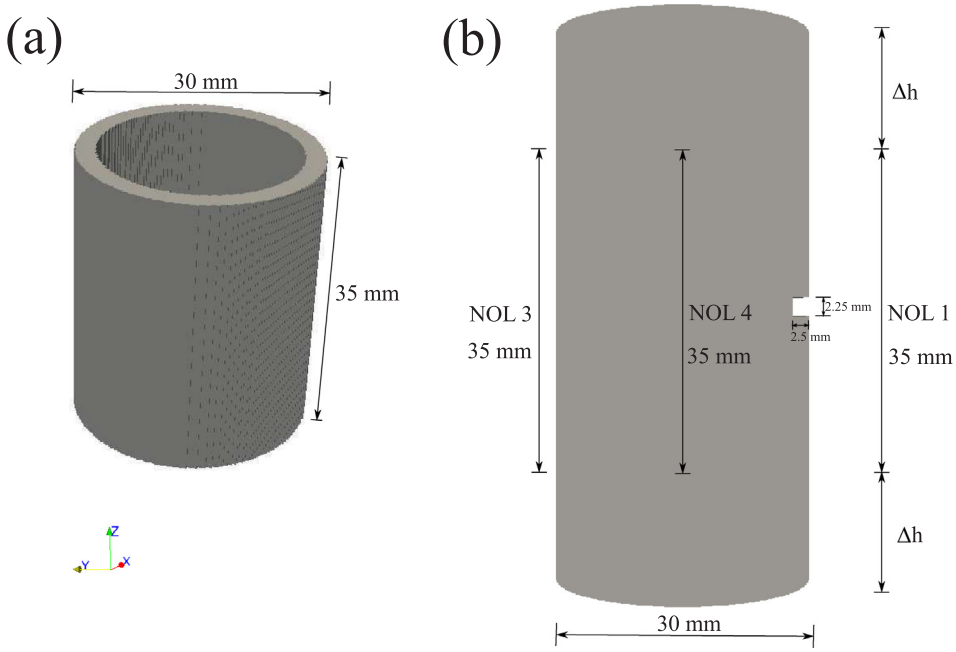

Fig. 3. Cell-based images of the structure of cement paste pipes for uniaxial tensile simulations. (a) Unnotched pipe and (b) single notched pipe (NOL represents numerical output location, considering LVDT used in Fig. 1b).

Table 1
Experimental results of global mechanical properties of unnotched cement paste pipes (Fig. 1a).

Specimen number	Young's modulus (GPa)	Tensile strength (MPa)
Specimen 1	20.9	5.6
Specimen 2	20.3	5.7
Specimen 3	19.7	5.7
Average	20.3	5.7

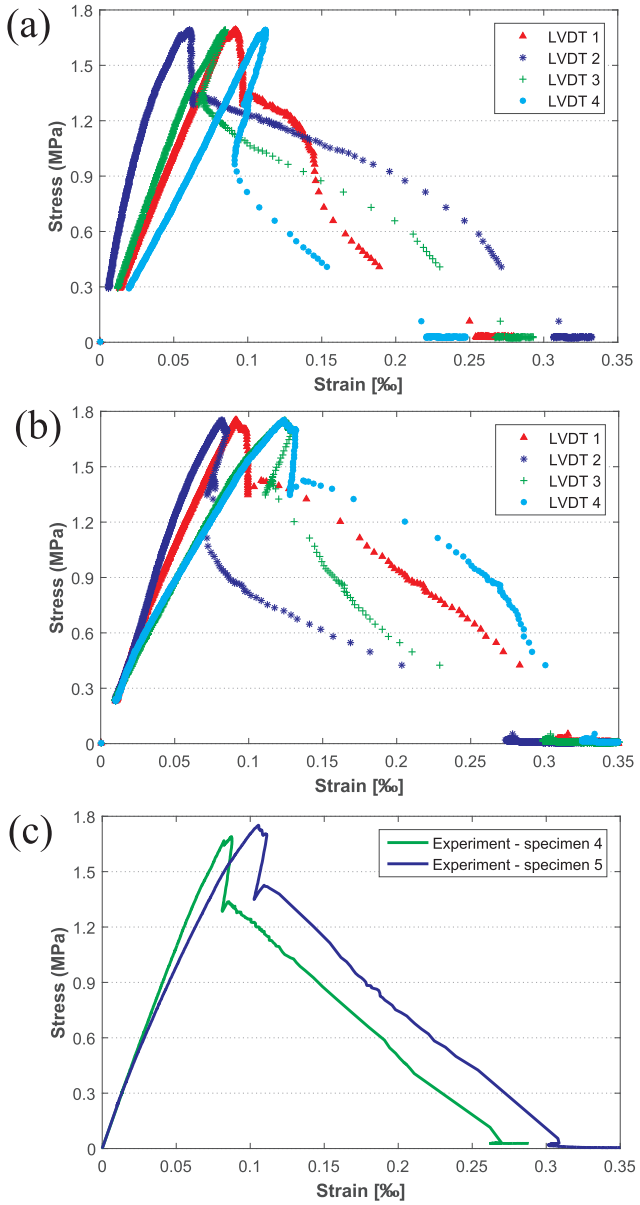

Fig. 4. Experimental stress-strain responses of single notched cement paste pipes (Fig. 1b) subjected to uniaxial tensile loading along vertical direction. (a) Specimen 4, (b) specimen 5 and (c) comparison between specimen 4 and specimen 5 (strain is the average value of the four LVDTs).

In addition to the experiments, a 3D lattice model was constructed to simulate the two types of specimens under the uniaxial tensile loading. The simulated stress-strain responses and cracking process were compared with the experimental observations. This part aims at studying the local mechanical properties of lattice elements, which is the input parameters of the simulations. An assumed value of the local mechanical properties for the lattice elements can result in a certain mechanical response for the simulated specimen. Therefore, the local mechanical properties with softening information for lattice elements can be obtained when simulated specimen response matched with the experimental observations. It has been long known that strength and facture behaviour of quasi-brittle materials is size dependent [8]. The tensile strength of cement paste increases when its size becomes smaller [9]. In the simulations, the specimen is represented by a network of lattice elements. Therefore, the specimen and the lattice element represent the same material but have different size. The aim of the simulations in this study is to obtain the local mechanical properties of the lattice elements (mesh size) based on the global mechanical properties of the specimens (experimental observations).

These specimens were chosen in this study as them were used to investigate the degradation caused by external sulfate attack [10,11]. In order to be able to simulate the degradation process, the essential mechanical properties of the unexposed specimens are required, which were studied in this paper.

2. Materials and methods

2.1. Materials and specimens

An ordinary Portland cement (CEM I 42,5 N) with a water/cement ratio of 0.40 was used in this study. PVC moulds with stainless steel rods in the center were fabricated in order to produce the cement paste pipes with a wall thickness of 2.5 mm (outer diameter 30 mm, inner diameter 25 mm). More information regarding the experimental setup can be found in Ma et al. [10,11]. After 60-day curing in saturated limewater, the cement paste pipes were cut and polished at both ends to ensure that they were parallel and that the length was 35 mm. Then the prepared specimens were put back to the saturated limewater.

Two types of specimens were tested, which were the unnotched cement paste pipes (Fig. 1a) and single notched cement paste pipes (Fig. 1b). For the single notched specimen, a notch with a depth of 2.5 mm and a width of 2.25 mm was sawn at one side of the specimen at half-height (Fig. 2). After that, the prepared specimens were put back to the saturated limewater.

After 90-day curing in saturated limewater, all specimens were taken out of limewater for uniaxial tensile tests. In order to prevent drying cracks, the specimens were wrapped with plastic foil during the entire test procedure (Fig. 1). In addition, a sponge, which was saturated with water, was also put inside the hollow part of the specimens to minimize drying. The plastic foil was removed when the test was finished, as shown in Fig. 2b.

2.2. Uniaxial tensile test

Uniaxial tensile tests were performed in an Instron 8872 servo-hydraulic system. The specimens were glued between steel platens of the testing machine and loaded in deformation control.

For the unnotched cement paste pipes (Fig. 1a), the tests were controlled by the average value of the four linear variable differential transducers (LVDTs) at a constant loading speed of 0.2 μm/s.

For the single notched cement paste pipes (Fig. 1b), the tests were firstly controlled by LVDT 1 at a constant loading speed of 0.02 μm/s. LVDT 1 was located at the side of the notch. Afterwards, when the stress-strain curve passed the peak, the tests were changed to be controlled by the average value of the four LVDTs.

2.3. Lattice fracture model

Fracture processes of cementitious materials can be studied with the Delft lattice model [12]. In this model, material is discretized as a network of beam elements which can transfer forces. The fracture process is simulated by the removal of lattice elements step by step. At every analysis step, a prescribed displacement is imposed on the lattice

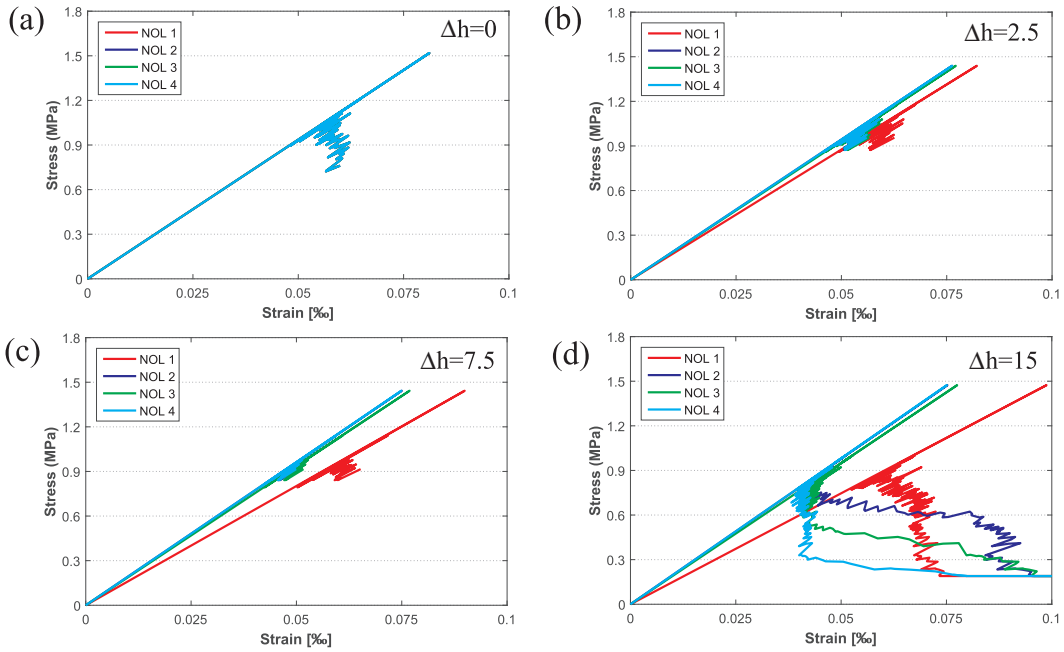

Fig. 5. Influence of increased height (Δh), which is corresponding to Fig. 3b. Simulated stress-strain responses of the single notched cement paste pipe (Fig. 3b) subjected to uniaxial tensile loading along vertical direction. Lattice elements behave as linear elastic (Fig. 6a). (a) $\Delta h = 0$ mm, (b) $\Delta h = 2.5$ mm, (c) $\Delta h = 7.5$ mm and (d) $\Delta h = 15$ mm.

structure to find one critical element that has the highest stress/strength ratio, and then removing it from the system or changing it to have a weaker mechanical property. The basic removal procedure is to remove one element at one lattice analysis step. In the case of implementing local softening behavior, the strength and stiffness of each element are decreased step by step. The analysis procedure is repeated until a pre-determined failure criterion is achieved, such as a certain value of the displacement. The lattice element can fail only in tension. This method can simulate crack propagation, and thus, predict the global stress-strain response [13]. Details about the complete computational procedure and the equations of the model are available in the literature [14].

Two types of uniaxial tensile tests were simulated which corresponds to the experiments. The first type is the uniaxial tensile simulation of the unnotched cement paste pipe, as shown in Fig. 3a. The wall thickness of the pipe is 2.5 mm (outer diameter 30 mm, inner diameter 25 mm) and the length is 35 mm, which is the same as in the experiment (Fig. 1a).

The second type is the uniaxial tensile simulation of the single notched cement paste pipe (Fig. 3b). During the experiments, since the rotational stiffness of the steel platens of the testing machine were not infinitely stiff, the plane of the specimen boundary can rotate, which leads to the differences of the deformations of the four LVDTs. However, in the modelling, the plane of the specimen boundary will not rotate. In order to take the rotations into account, it was chosen to increase the height of the specimen in the modelling. As shown in Fig. 3b, "Δh" represents the increased height. In this case, during the simulations, the plane of the specimen boundary will not rotate. However, the plane of "the middle part" (NOL part) boundary can rotate, which results in a similar behaviour as in the experiments. Four locations were chosen at the simulated structure, which were the same as the locations of LVDTs in the experiments. For each location, two nodes were chosen, which were along the same vertical line. The distance between the two nodes is expressed as NOL. The original NOL is 35 mm, which is same as the length of the LVDTs in the experiments (Fig. 1b). During the simulations, the change of NOL was recorded. A single notch with the depth of 2.5 mm and the thickness of 2.25 mm was also applied at the half-height of the simulated pipe, which was similar to the experimental setup. NOL 1 was located at the side of the notch.

The specimens were meshed at the resolution of 0.25 mm/cell, and a 3D quadrangular lattice network was constructed. A sub-cell was created within each cell sharing the same center, and the length ratio of the sub-cell to the cell is defined as randomness. The value of randomness is always between 0 and 1 [15]. More details about the influence of randomness can be found in [16]. A lattice node was positioned within the cell randomly and neighbor nodes were connected by a lattice element. During the 3D mesh generation process, the randomness of the lattice system was set to 0.5 for all the non-boundary cells and 0 for all the boundary cells. The randomness of 0.5 can introduce irregular geometry of the mesh. The cross-section of the lattice element was assumed to be circular and was chosen such that the stiffness of the system is equal to the stiffness of the local element. For all the simulations in this section, all the lattice elements were assumed to have the same local mechanical properties.

3. Experimental results and discussion

3.1. Unnotched cement paste pipes

Three unnotched cement paste pipes (specimen 1, 2 and 3) were tested in uniaxial tension, as shown in Fig. 1a. The Young's modulus of 20.3 GPa and tensile strength of 5.7 MPa were found, as presented in Table 1. However, the tests stopped immediately after the peak stress of the stress-strain curve. The tests were controlled by the average deformation of the four LVDTs. Before the peak stress, the average deformation kept increasing. However, after the peak stress, the average deformation began to decrease. Increasing deformation is needed as feedback signal to perform a stable test. Therefore, after the peak stress, a sudden failure of the specimen occurred. The reasons are discussed in detail in Section 3.3. In this case, the post-peak stress-strain curve cannot be measured if the unnotched specimens were chosen.

3.2. Single notched cement paste pipes

Two single notched cement paste pipes (specimen 4 and 5) were

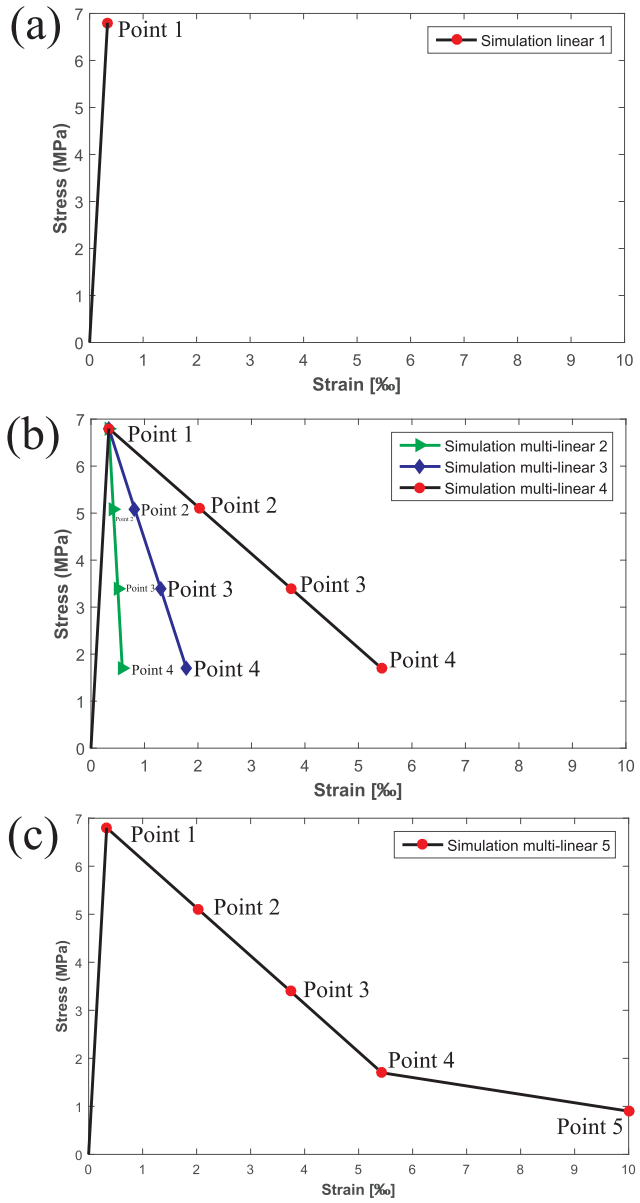

Fig. 6. Assumed local mechanical properties of lattice elements. (a) Simulation linear 1 (linear elastic behavior), (b) simulation multi-linear 2, 3, 4 (multi-linear behavior) and (c) simulation multi-linear 5 (multi-linear behavior).

tested in uniaxial tension, as shown in Fig. 1b. The stress-strain responses with post-peak softening information are presented in Fig. 4. As can be found in Fig. 4a, after reaching the peak stress, LVDT 1 and LVDT 2 kept increasing, and LVDT 3 and LVDT 4 started to decrease, which was due to the localization of cracking. The tests changed to the stage of unloading after reaching peak stress. Because of the decrease of applied tensile load, the deformation of uncracked part also decreased, which lead to the snap back phenomenon (LVDT 3 and LVDT 4). The main crack started from the notch tip, which was located either between LVDT 1 and LVDT 2 or between LVDT 1 and LVDT 4. In Fig. 4a, LVDT 1 and LVDT 2 continued increasing after peak stress, therefore the main crack started at the notch tip between LVDT 1 and LVDT 2. After peak stress, both of LVDT 3 and LVDT 4 decreased firstly and then increased. LVDT 3 increased earlier. Therefore, the main crack continued to develop and passed the location of LVDT 3. After that, another main crack started at the other notch tip between LVDT 1 and LVDT 4. Since these two main cracks were at two different planes, an inclined plane connected these two cracks and the whole specimen was fractured finally, as presented in Fig. 2b. In specimen 5, the crack propagates in the opposite direction as can be seen in Fig. 4b.

3.3. Discussion

The experimental results have shown that it was possible to obtain the softening behavior of the very brittle cement paste pipes when a notch was introduced.

For the notched specimens, the main crack started from the notch (Section 3.2). The tests were controlled by LVDT 1, which was located at the side of the notch. During the tensile tests, LVDT 1 kept increasing until the end, even though the other three LVDTs may decrease after peak stress, as can be found in Fig. 4a and b. It can be seen that the average of the four LVDTs began to decrease after peak stress. For the deformation controlled tensile tests, the increase of deformation is needed for a stable test. If the tests of the single notched specimens are controlled by the average of the four LVDTs, the post-peak stress-strain curve can still not be obtained due to deformation decrease.

For the unnotched specimens in Section 3.1, the location for crack nucleation and growth is unknown. Therefore, the tests were controlled by the average of the four LVDTs, which started to decrease after peak stress. As a result, the post-peak stress-strain curve cannot be obtained during the experiments.

4. Numerical simulation results and discussion

4.1. Unnotched cement paste pipe

As mentioned in Section 3.1, the Young's modulus of 20.3 GPa and tensile strength of 5.7 MPa were found experimentally for the unnotched specimens.

For the simulations, a value of 20.3 GPa was chosen as the Young's modulus of the lattice elements. The cross section of the lattice elements was adjusted so that the global Young's modulus of the specimen was also 20.3 GPa. However, the tensile strength of the lattice elements needs to be determined through inverse modelling.

A linear elastic behavior for the lattice elements was assumed. The external tensile loading was imposed on the top and bottom surfaces in the z-direction (Fig. 3a). It was found that the global tensile strength of 5.7 MPa for the specimen could be achieved when the local tensile strength of 6.8 MPa was applied on the lattice elements.

In that way, the Young's modulus and tensile strength of lattice elements were obtained based on the experimental results, which are presented as point 1 in Fig. 6.

4.2. Single notched cement paste pipe

This section discusses the simulations of the single notched specimen (Fig. 3b). The external tensile loading was imposed on the top and bottom surfaces in the z-direction. The linear elastic part of lattice elements was obtained in Section 4.1 (point 1 in Fig. 6). In this section, the softening part of lattice elements is discussed.

4.2.1. Influence of increased height of simulated structure

As discussed in Section 2.3, in order to simulate the situation in experiments, the length of the simulated pipe was chosen to be larger. The increased height is expressed as "Δh" (Fig. 3b). The Young's modulus and tensile strength of lattice elements were chosen as 20.3 GPa and 6.8 MPa, respectively, as shown in Fig. 6a.

The simulated stress-strain responses of specimens with different increased height (Δh) are shown in Fig. 5. As can be found in Fig. 5a, when the height of the simulated pipe was the same as the experiments, the responses of the four NOLs were also the same. When the increased height (Δh) was above 0, the responses of the four NOLs started to be different. A larger increased height (Δh) can lead to a greater difference among the four NOLs. In experiments, the strain of LVDT 1 at peak load

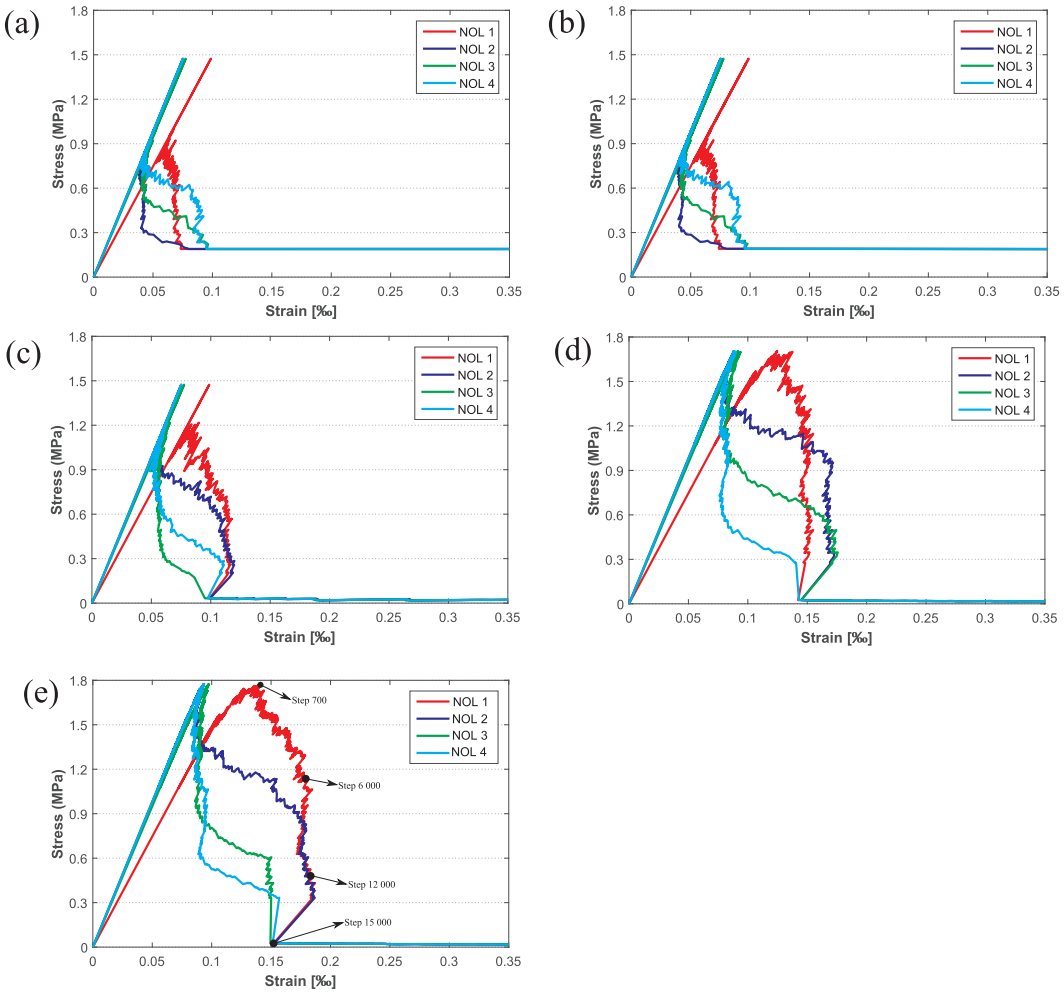

Fig. 7. Simulated stress-strain responses of the single notched cement paste pipe (Fig. 3b, $\Delta h = 15$ mm) subjected to uniaxial tensile loading along vertical direction. The local mechanical properties of lattice elements are referred to Fig. 6. (a) Simulation linear 1, (b) simulation multi-linear 2, (c) simulation multi-linear 3, (d) simulation multi-linear 4 and (e) simulation multi-linear 5.

was close to 0.1‰ (Fig. 4a and b). In Fig. 5d, the strain of NOL 1 at peak load was also close to 0.1‰. Therefore, $\Delta h = 15$ mm was chosen for the following simulations.

4.2.2. *Influence of local mechanical properties of lattice elements*

Five simulations were carried out. The linear elastic behavior was used for the lattice elements in "simulation linear 1". For the other four simulations, the softening behavior was applied on the lattice elements. The assumed local mechanical properties were shown in Fig. 6. Point 1 in Fig. 6a, b and c are even, which was obtained in Section 4.1. The other points were assumed, which formed a multi-linear curve for each case. One more point was added on "simulation multi-linear 4" to form "simulation multi-linear 5".

The simulated stress-strain responses of the specimen are presented in Fig. 7. The softening behavior of the specimen closer to the experimental result can be obtained by changing the local softening behavior of lattice elements, as presented in Fig. 7e.

Furthermore, the comparisons between experimental and simulated stress-strain responses of the specimen are summarized in Fig. 8. The strain in the curves stands for average strain of the four LVDTs or NOLs. The corresponding local mechanical properties applied on lattice elements are shown in Fig. 6. The softening part of the simulated curves is quite different among the simulations (Fig. 8f). Fig. 8e shows the best simulated results compared with the other four simulations, and matches the experimental curves. To some extents, by changing the shape of the softening part of local mechanical properties, an even better match can be obtained.

The fracture energy of experiments and lattice elements with assumed local mechanical properties is listed in Table 2, which was calculated as the length in the loading direction multiplied by the area below the stress-strain curve (Fig. 4c and Fig. 6) [17]. The length of 35 mm was used for calculations in experiments, and the length of 0.25 mm was assumed for calculations in lattice elements. It can be found that the fracture energy of "simulation multi-linear 5" is similar as the fracture energy of experiments. Therefore, if the fracture energy of lattice elements with assumed local mechanical properties is closed to the fracture energy of experiments, the simulated stress-strain responses of the specimen is also close to the curves measured by experiments.

The simulated cracking process caused by uniaxial tensile loading are shown in Fig. 9. Fig. 6c was used as the local mechanical properties of lattice elements. The corresponding stress-strain response at certain analysis step is marked in Fig. 7ted in Fig. 9, it is found that the crack first started at the notch between NOL 1 and NOL 2. Then another crack started at the notch between NOL 1 and NOL 4. Finally, these two cracks met at the location between NOL 3 and NOL 4. As can be seen, these two cracks were at two different planes, therefore, an inclined plane made these two cracks connect. As shown in Fig. 7k stress, NOL 1 continued to increase, however, the other three NOLs started to decrease. Afterwards, NOL 2 first started to increase, followed by NOL 3 and then NOL 4. That also indicated that the crack first started at the notch between NOL 1 and NOL 2. It can be concluded that the

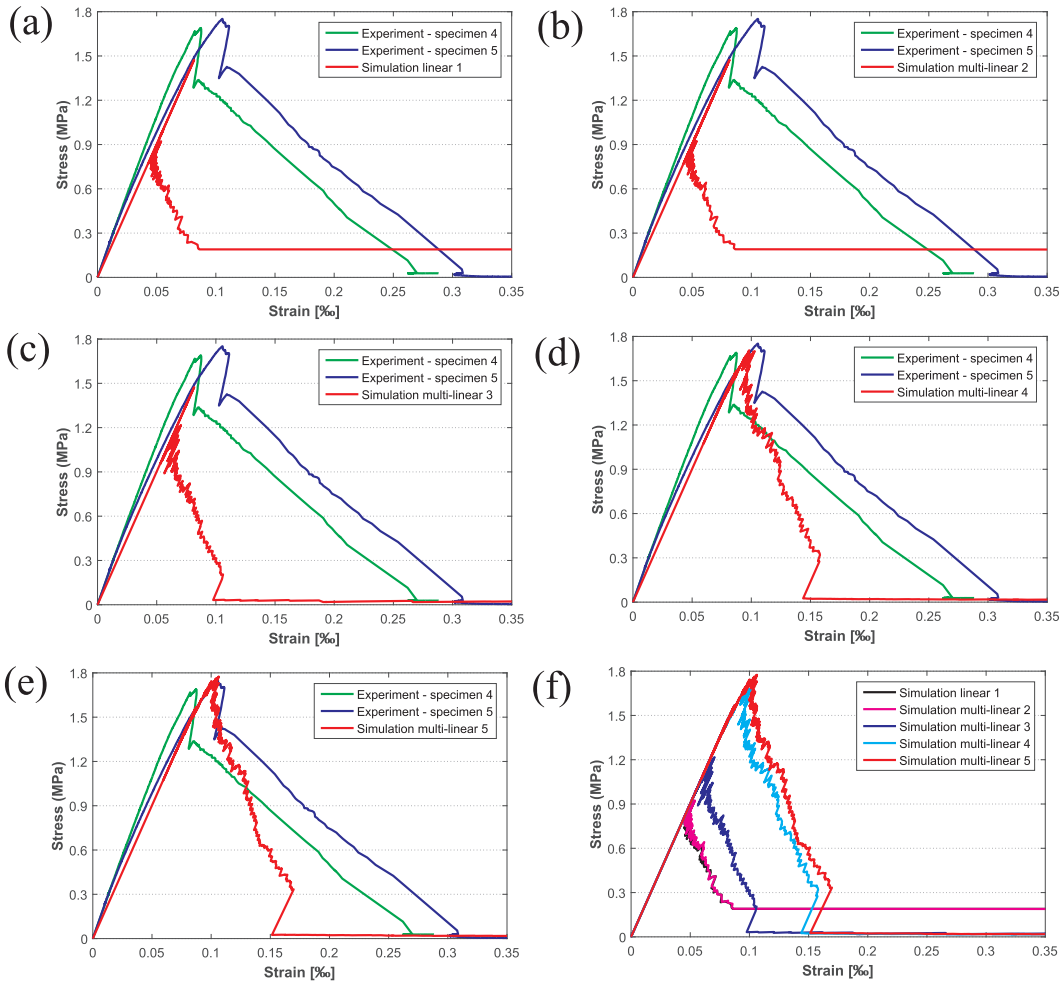

Fig. 8. Results of the single notched cement paste pipe (experiment: Fig. 1b, simulation: Fig. 3b, $\Delta h = 15$ mm) subjected to uniaxial tensile loading along vertical direction. Strain is the average value of the four LVDTs or NOLs. Comparisons between experimental and simulated stress-strain responses (a) simulation linear 1, (b) simulation multi-linear 2, (c) simulation multi-linear 3, (d) simulation multi-linear 4, (e) simulation multi-linear 5 and (f) comparisons among simulated stress-strain responses.

Table 2
Calculations of fracture energy.

		Fracture energy (J/m^2)
Lattice elements with assumed local mechanical properties, corresponding to Fig. 6	Simulation linear 1	0.3
	Simulation multi-linear 2	0.6
	Simulation multi-linear 3	1.8
	Simulation multi-linear 4	5.7
	Simulation multi-linear 5	7.2
Experimental results, corresponding to Fig. 4c	Experiment - specimen 4	7.1
	Experiment - specimen 5	8.9

simulated cracking process is similar to the experimental observation.

4.3. Discussion

The linear elastic part of lattice elements (Fig. 6a) was obtained after simulations of the unnotched specimen. Afterwards, based on simulations of the single notched specimen, the softening part of lattice elements was suggested, as shown in Fig. 6c. When the curve in Fig. 6c was used for the local properties of the lattice elements for the unnotched specimen, this has an influence on the tensile strength of the specimen. Because part of the material is most probably already in the softening regime when the peak load is reached. It was found that the simulated tensile strength of the specimen is 6 MPa, which is just a slight increase of the tensile strength.

5. Conclusions

In this study, cement paste pipes with a wall thickness of 2.5 mm and a water/cement ratio of 0.40 were used. The uniaxial tensile tests were carried out on specimens after 90-day limewater curing. The mechanical properties of the unnotched and single notched specimens were investigated experimentally and numerically. Firstly, a uniaxial tensile loading was applied on unnotched specimens along longitudinal direction. A Young's modulus of 20.3 GPa and tensile strength of 5.7 MPa were found. However, the softening behavior of the specimen cannot be obtained, because the material is too brittle. After that, the

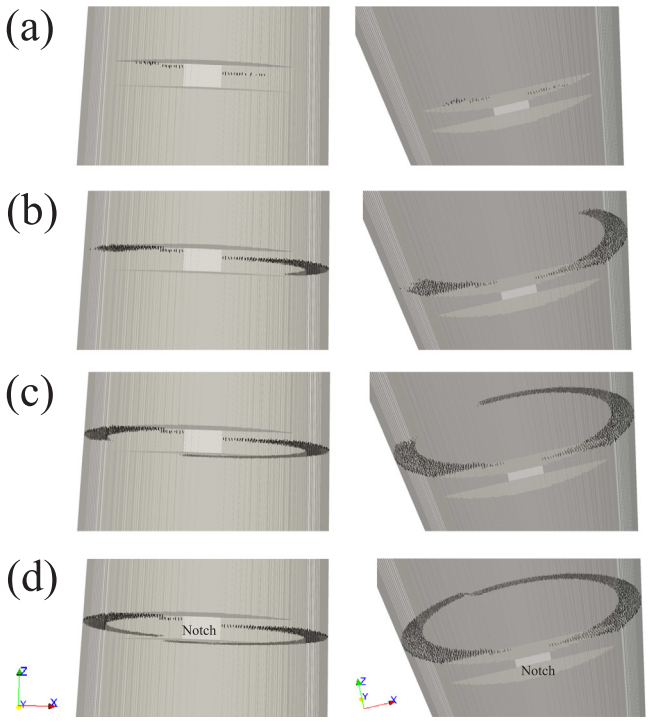

Fig. 9. Simulated crack patterns of the single notched cement paste pipe subjected to uniaxial tensile loading along vertical direction at (a) step 700, (b) step 6 000, (c) step 12 000 and (d) step 15 000 (black-damaged element), corresponding to Fig. 7nsileSimulationCrackPattern.

specimens with a notch were also subjected to uniaxial tensile loading. A single notch was sawn at one side of the specimens at half-height, which can trigger crack growth from a known location. Therefore, the complete stress-strain responses with softening information were obtained.

A 3D lattice model with a mesh resolution of 0.25 mm/cell was constructed to simulate the stress-strain responses measured by uniaxial tensile experiments. A single notch was also applied at the half-height of the simulated pipe, which was the same as the experimental setup. Both of the unnotched and single notched specimens were simulated. The local mechanical properties of lattice elements were discussed. After the tensile simulations of the unnotched specimen, the Young's modulus of 20.3 GPa and tensile strength of 6.8 MPa were obtained for lattice elements. Afterwards, the softening behavior of lattice elements was studied by the tensile simulations of the single notched specimen. The mechanical properties which behave as a multi-linear curve were achieved for lattice elements. The simulated stress-strain responses of the four NOLs and cracking process were compared with the experimental observations. It was found that the simulated results matched quite well with the experiments.

Performing fracture tests on extremely brittle material, like the cement paste used in this study, is quite difficult. In this paper, a method to perform such tests by using notched and unnotched specimens is shown. From these tests, local mechanical properties could be fitted that are used in simulations with a discrete element (lattice) model. This simulation method is further used to perform predictions of cement paste specimens with a similar geometry exposed to external sulfate attack. More details can be found in Ma [18].

Acknowledgements

The scholarship from the Oversea Study Program of Guangzhou Elite Project is gratefully acknowledged.

References

[1] J. Van Mier, M. Van Vliet, Uniaxial tension test for the determination of fracture parameters of concrete: state of the art, Eng. Fract. Mech. 69 (2) (2002) 235–247.
[2] H. Toutanji, L. Liu, T. El-Korchi, The role of silica fume in the direct tensile strength of cement-based materials, Mater. Struct. 32 (3) (1999) 203.
[3] B. Hughes, G. Chapman, The complete stress-strain curve for concrete in direct tension, RILEM Bull. 30 (1966) 95–97.
[4] R. Evans, M. Marathe, Microcracking and stress-strain curves for concrete in tension, Matériaux et Construct. 1 (1) (1968) 61–64.
[5] E. Schlangen, J. Van Mier, Experimental and numerical analysis of micromechanisms of fracture of cement-based composites, Cement Concr. Compos. 14 (2) (1992) 105–118.
[6] D.A. Hordijk, Local approach to fatigue of concrete, PhD thesis Delft University of Technology, Delft, The Netherlands, 1991.
[7] J.G. Van Mier, M. Nooru-Mohamed, Geometrical and structural aspects of concrete fracture, Eng. Fract. Mech. 35 (4–5) (1990) 617–628.
[8] Z.P. Bažant, Size effect, Int. J. Solids Struct. 37 (1–2) (2000) 69–80.
[9] H. Zhang, B. Šavija, Y. Xu, E. Schlangen, Size effect on splitting strength of hardened cement paste: Experimental and numerical study, Cement Concr. Compos. 94 (2018) 264–276.
[10] X. Ma, O. Çopuroğlu, E. Schlangen, N. Han, F. Xing, Experimental and numerical study on cement paste degradation under external sulfate attack, Proceedings of 9th International Conference on Fracture Mechanics of Concrete and Concrete Structures, 2016.
[11] X. Ma, O. Çopuroğlu, E. Schlangen, N. Han, F. Xing, Expansion and degradation of cement paste in sodium sulfate solutions, Constr. Build. Mater. 158 (2018) 410–422.
[12] E. Schlangen, Experimental and numerical analysis of fracture processes in concrete, PhD thesis Delft University of Technology, Delft, The Netherlands, 1993.
[13] E. Schlangen, E. Garboczi, Fracture simulations of concrete using lattice models: computational aspects, Eng. Fracture Mech. 57 (2) (1997) 319–332.
[14] E. Schlangen, Z. Qian, 3d modeling of fracture in cement-based materials, J. Multiscale Modell. 1 (02) (2009) 245–261.
[15] Z. Qian, E. Schlangen, G. Ye, K. van Breugel, Modeling framework for fracture in multiscale cement-based material structures, Materials 10 (6) (2017) 587.
[16] Z. Qian, Multiscale modeling of fracture processes in cementitious materials, PhD thesis Delft University of Technology, Delft, The Netherlands, 2012.
[17] F. Wittmann, H. Mihashi, N. Nomura, Size effect on fracture energy of concrete, Eng. Fract. Mech. 35 (1–3) (1990) 107–115.
[18] X. Ma, Cement paste degradation under external sulfate attack: An experimental and numerical research, PhD thesis Delft University of Technology, Delft, The Netherlands, 2018.